# Studies of CW Laser Oscillation on the 1315-nm Transition of Atomic Iodine Pumped by $O_2(a^1\Delta)$ Produced in an Electric Discharge

David L. Carroll, *Member, IEEE*, Joseph T. Verdeyen, *Life Senior Member, IEEE*, Darren M. King, Joseph W. Zimmerman, Julia K. Laystrom, Brian S. Woodard, Gabriel F. Benavides, Nathan R. Richardson, Kirk W. Kittell, and Wayne C. Solomon

***Abstract*—In this paper, we report on studies of a continuous-wave laser at 1315 nm on the $I(^2P_{1/2}) \rightarrow I(^2P_{3/2})$ transition of atomic iodine where the $O_2(a^1\Delta)$ used to pump the iodine was produced by a radio frequency excited electric discharge. The electric discharge was sustained in He–$O_2$ and Ar–$O_2$ gas mixtures upstream of a supersonic cavity which is employed to lower the temperature of the continuous gas flow and shift the equilibrium of atomic iodine in favor of the $I(^2P_{1/2})$ state. The results of experimental studies for several different flow conditions, discharge arrangements, and mirror sets are presented. The highest laser output power obtained in these experiments was 520 mW in a stable cavity composed of two 99.995% reflective mirrors.**

***Index Terms*—Chemical oxygen–iodine laser (COIL), electric discharge oxygen–iodine laser, electriCOIL, radio frequency (RF) excitation of oxygen, singlet-delta oxygen.**

## I. Introduction

The classic chemical oxygen–iodine laser (COIL) system [1] operates on the $I(^2P_{1/2}) \rightarrow I(^2P_{3/2})$(hereafter denoted as I* and I, respectively) electronic transition of the iodine atom at 1315 nm. The population inversion relies on the near resonant energy transfer from the excited singlet oxygen molecule, $O_2(a^1\Delta)$ (denoted $O_2(a)$ hereafter) to the upper spin-orbit level $^2P_{1/2}$ of atomic iodine, I*. Conventionally, $O_2(a)$ is produced by a liquid chemistry singlet oxygen generator (SOG). There are many system issues having to do with weight, safety and the ability to rapidly modulate the production of the $O_2(a)$ which have motivated investigations into methods to produce $O_2(a)$ using flowing electric discharges. Early attempts to implement electric discharges to generate $O_2(a)$ and transfer to iodine to make a laser by Zalesskii and Yu [2] and Fournier *et al.* [3] did not result in positive gain. Over the past several years, investigations into the possibility of a hybrid electrically powered oxygen–iodine laser have been performed with electric discharges to produce the $O_2(a)$ [4]–[9]. These studies have shown that flowing electric discharges through oxygen containing mixtures, typically diluted with a rare gas, can produce quantities of $O_2(a)$ that can be sufficient for lasing under certain conditions. Recent studies have demonstrated $O_2(a)$ yields greater than 15% using electric discharges [6], [7], [9], and modeling results [4], [7], [8], [10] indicated that such a system could produce a viable laser. Recently, Carroll *et al.* [11], [12] reported direct measurements of positive gain in atomic iodine resulting from electric discharge produced $O_2(a)$ followed by a lasing demonstration [13]. Following the measurement of positive gain in a supersonic flow [11], Rawlins *et al.* [14] measured positive gain in a higher temperature subsonic flow.

Manuscript received April 27, 2005; revised June 16, 2005. This work was supported in part by the Air Force Office of Scientific Research (AFOSR) and by the Missile Defense Agency (MDA) through the U.S. Army Space and Missile Defense Command (USA SMDC).

D. L. Carroll, J. T. Verdeyen, D. M. King, J. W. Zimmerman, and J. K. Laystrom are with CU Aerospace, Champaign, IL 61820 USA (e-mail: carroll@cuaerospace.com).

B. S. Woodard, G. F. Benavides, N. R. Richardson, K. W. Kittell, and W. C. Solomon are with the University of Illinois, Urbana, IL 61801 USA.

Digital Object Identifier 10.1109/JQE.2005.854316

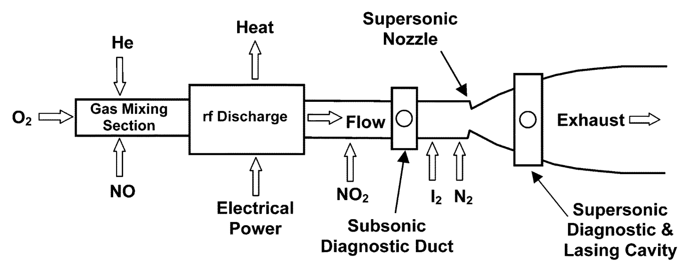


Fig. 1. Schematic of the experimental apparatus.

## II. Experimental Setup

A block diagram of the flow tube setup is shown in Fig. 1. Three different discharge configurations were tested as the excitation source. All of the discharges employed a radio frequency (RF) electric discharge at 13.56 MHz. The variation in configurations will be discussed at more length in Sections IV-A–C.

The supersonic diagnostic cavity has a Mach 2 nozzle with windows that serve as view ports. Upstream of the nozzle, the subsonic diagnostic duct has four windows through which simultaneous measurements are made of the optical emission from $O_2(a)$ at 1268 nm and $O_2(b^1\Sigma)$ [denoted $O_2(b)$ hereafter] at 762 nm. A Roper scientific optical multichannel analyzer (OMA-V) with a 512-element InGaAs $LN_2$ cooled array interfaced to an Acton Research SP-150 monochromator, was used for measurements at 1268 nm. (Note that the presence of NO and/or $NO_2$ added a broad-band background "airglow" emission signal that was subtracted out during post-processing of the 1268-nm OMA-V measurements.) A ST-6 charge-coupled device (CCD) camera from Santa Barbara Instruments Group, Inc. coupled to a Jarrell Ash M10 023 100 monochromator was implemented to measure the band emission of $O_2(b)$ at 762 nm. By using published values of the line strengths for the P, Q, PQ, R, and RQ branches and matching the experimental spectra to the theoretical one, we obtain a spectroscopic measurement of the gas temperature [5].

Micro-Motion CMF and Omega FMA mass flow meters were used to measure the flow rates of the gases. A pair of Micro-Motion CMF-025's were used to measure the $O_2$ and $N_2$ flow rates, a Micro-Motion CMF-010 to measure the primary He flow rate, an Omega FMA3109 to measure the NO flow, an Omega FMA3108 to measure the secondary He flow that carries the $I_2$, and an Omega FMA3107 to measure the $NO_2$ flow. The $I_2$ concentration was measured by a method developed by Physical Sciences Inc. (PSI) and is based on the continuum absorption of molecular iodine at 488 nm. Details of this diagnostic are described by Rawlins *et al.* [15]. Pressure in the subsonic and supersonic flow regions were measured by capacitance manometers from MKS (model 124AA-00 100AB-S) and Leybold (model CM10). Incident and reflected powers from the RF matching network were measured by a Bird Thruline model 43 wattmeter (RF "System Power" is the difference of the incident and reflected powers). $V$–$I$ characteristics were taken with a capacitance divider voltage probe and a Pearson Model 480 current monitor. Note that RF system power is presented in the plots; separate electrical measurements indicate that approximately 80%–90% of the system power is actually absorbed by the plasma for the $O_2$–He mixtures we ran in these experiments for both the longitudinal and inductive discharges. For example, for an RF power of 500 W, the absorbed power by the plasma was approximately 425 W (85% of 500 W), and the remainder of the power was lost to electrical line losses.

Measurements of gain (or absorption) were made using the Iodine-Scan Diagnostic (ISD) developed by PSI [16] prior to installing the laser mirrors. The ISD is a diode laser-based monitor for the small signal gain in iodine lasers. The system uses a single mode, tunable diode laser that is capable of accessing all six hyperfine components of the atomic iodine. It was calibrated in frequency to enable automated operation for the (3,4) hyperfine transition for our experiments. A fiber-optic cable was used to deliver the diode laser probe beam to the iodine diagnostic regions in the subsonic portion of the flow tube and in the supersonic cavity. Since the ISD uses a narrow band diode laser, measurements of the lineshapes can also be used to determine the local temperature from the Voigt profile.

The windows on the sides of the cavity when using the gain diagnostic were wedged and antireflection coated to minimize etalon effects. A four-pass configuration (20-cm path length) was used for the gain measurements in the supersonic section. Measurements of the $O_2(a)$ yield {defined as $Y = O_2(a)/[O_2(X) + O_2(a)]$} were obtained from the $O_2(a)$ signal measurements made by the OMA-V that were previously calibrated to gain measurements [12], using techniques originally developed by Hager [17], Davis and Rawlins [15]. [Note that $O_2(X)$ is used here as an abbreviation for the $O_2(X^3\Sigma)$ ground state of oxygen].

Laser power measurements were made with a Scientech Astral model AC2500/AC25H calorimeter interfaced to a Scientech Vector model S310 readout, and were made at the same location in the supersonic laser cavity as were the gain measurements. The gain measurements were made first. The vacuum mirror mounts were then installed for the laser power trials. Different sets of mirrors (discussed in Section III) formed a stable optical cavity. The mirrors were separated by 38 cm. An infrared (IR) detection card from New Focus, Model 5842, with response between 800–1600 nm, was also used to observe the intensity profile of the beam.

TABLE I
MEASUREMENTS OF MIRROR TRANSMISSIVITY AND ESTIMATED REFLECTIVITY FROM $1 - T$. NOTE THAT CC INDICATES A CONCAVE MIRROR

| Mirror # | Curvature | Manufacturer | Transmissivity, T | Reflectivity, R |
|---|---|---|---|---|
| 1 | 1m CC | LGR | 0.000135 | 0.999865 |
| 2 | 1m CC | LGR | 0.000143 | 0.999857 |
| 3 | 2m CC | LGR | 0.000071 | 0.999929 |
| 4 | 2m CC | LGR | 0.000070 | 0.999930 |
| 7 | 2m CC | ATF | 0.000053 | 0.999947 |
| 8 | 2m CC | ATF | 0.000051 | 0.999949 |

## III. Mirror Selection and Measurements

The choice of mirror reflectivities was based on previous measurements of gain. For laser oscillations to occur, the gain coefficient at line center $\gamma_0(\nu_0)$ must satisfy

$$\gamma_0(\nu_0) \geq \frac{1}{2l_g} \ln\left(\frac{1}{R_1 R_2}\right) \equiv \gamma_{\text{th}}(\nu_0) \text{ (threshold)} \qquad (1)$$

where $l_g$ is the length of the gain medium (5 cm for our experiment) and $R_1$ and $R_2$ are the mirror reflectivities. For similar flow conditions we previously [12] obtained a gain of $\approx 0.005\%$ cm$^{-1}$. With these values of gain and gain length, laser oscillation requires mirrors having reflectivity exceeding $R_1R_2 = 0.999\,50$, or $R_1 = R_2 = 0.999\,75$. Based upon this requirement, mirrors were obtained having a reflectivity of $R > 0.9998$.

Different sets of mirrors with 1 and 2 m radii of curvature as well as two flats, were purchased from Los Gatos Research, Inc. (LGR) and AT Films (ATF). Table I lists measurements of the transmissivity $T$, from which the reflectivity $R$ was estimated as $1-T$. The transmissivity was determined by using the ISD laser diode and measuring the signal from an InGaAs detector coupled to a Stanford Research Systems Lock-in Amplifier Model SR530, with and without the mirror in the probe beam path. The probe beam signal for the transmission measurement was provided by the PSI gain diagnostic at 1315 nm. The transmission measurements were in close agreement with transmission curves provided by the manufacturers.

## IV. Experimental Results

Electric discharge stability and temperature control were found to be critical parameters to obtaining gain [11], [12]. Electric discharges sustained in moderate pressures (5–15 torr) of oxygen are prone to arcing and constriction. The production of O atoms, $O_3$ and other excited species by the discharge adds higher levels of complexity (these species are not encountered in the purely chemical system) to the downstream kinetics when the iodine donor species are added to the flow. The critical aspect of temperature control results from the equilibrium of the pumping reaction

$$O_2(a) + I \leftrightarrow O_2(X) + I^* \quad (2)$$

where the forward rate is $7.8 \times 10^{-11}$ cm$^3$/molecule $\cdot$ s [18], and the backward rate is $1.04 \times 10^{-10} \exp(-403/T)$ cm$^3$/molecule $\cdot$ s [19]. The equilibrium rate constant ratio of the forward to backward reactions is $K_{\rm eq} = [0.75 \exp(403/T)]$ [19], where $T$ is the gas temperature. The yield of $O_2(a)$ for optical transparency ($\gamma_{\rm OT} = 0$), also known as the "threshold yield", as a function of temperature is $Y_{\rm OT} = 1/[1 + 1.5 \exp(403/T)]$ [20]. Note, the backward rate is slower, $K_{\rm eq}$ larger, and $Y_{\rm OT}$ lower as $T$ is decreased.

### *A. Laser Performance With a Longitudinal RF Discharge*

The first type of discharge implemented for these lasing studies was a RF electric discharge at 13.56 MHz operated between two internal hollow cathode electrodes (each 10 cm long) oriented longitudinally in the same direction as the gas flow. For this longitudinal discharge, the plasma zone was approximately 4.9 cm in diameter and 25 cm long. Details of the performance of this electric discharge can be found in Carroll *et al.* [5]

Many flow conditions were investigated that resulted in gain and lasing using the configuration shown in Fig. 1. The experiments focused on a baseline case consisting of 3.0 mmol/s of $O_2$ mixed with 16.0 mmol/s of He running through the discharge. A tertiary flow of cold $N_2$ gas was injected further downstream to lower the temperature and to raise the pressure and mass flow rate to improve the performance of the nozzle with our vacuum system. The contour of the Mach 2 nozzle is similar to that given in [28]. Two adverse effects were believed to be occurring at low flow rates and pressures. First, the area ratio of this nozzle was a little too large for the pumps (two Roots MD-2700 blowers and a Kinney KT-850 single-stage rotary pump) to properly handle the lower pressure flow without the higher average molecular weight tertiary gas. Second, the nozzle performance was worse for low mass flow cases because of larger boundary layers in these cases. For illustrative purposes, if we take the standard expression for boundary layer displacement thickness [29] $\delta^* = 1.72\sqrt{\mu x/\rho U_0}$ (where $\mu$ is the gas viscosity, $\rho$ the mass density, $U_0$ the inlet flow velocity, and $x$ the distance in the flow direction), and substitute in the mass flow rate expression, $\dot{m} = \rho A U_0$ (where $A$ is the flow area), this gives

$$\delta^* = 1.72\sqrt{\frac{\mu x A}{\dot{m}}}. \quad (3)$$

At a fixed position in the nozzle, (3) shows how the boundary layer size is inversely proportional to the square root of the mass flow rate. As such, the addition of a large tertiary flow relative to the discharge flow will significantly reduce the size of the boundary layer for our flow conditions. (Note that (3) is only meant to be illustrative and breaks down as $x$ grows to large values, at which point the real flow field looks progressively more like a fully developed Poiseuille flow [30]). The combination of simultaneously raising pressure and mass flow rate by adding the higher average molecular weight tertiary gas helped to alleviate both of these adverse issues.

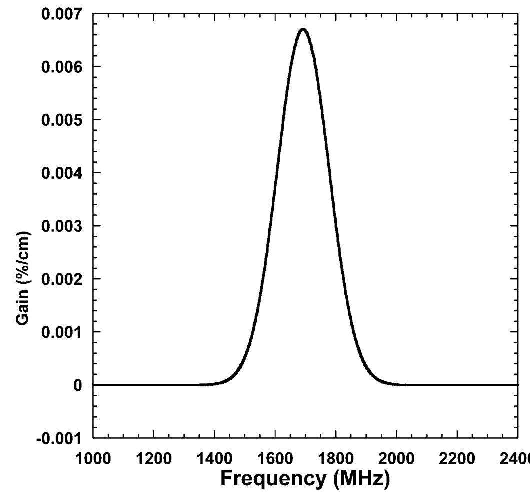


Fig. 2. Digitally filtered gain signal in the supersonic cavity as a function of laser diode scan frequency measured prior to lasing experiments.

The discharge production of $O_2(a)$ was enhanced by the addition of a small proportion of NO to lower the average ionization threshold and thereby also lower the sustaining value of $E/N$ of the gas mixture [12], therefore, most experiments were run with NO in the discharge. (NO has a lower ionization threshold than do $O_2$ and He, thus the addition of NO enhances the production of electrons, which increases the conductivity of the plasma, which reduces the electric field needed to sustain the plasma and consequently $E/N$ is reduced.) In earlier experiments that achieved positive gain using slightly different flow conditions, $NO_2$ was used to scavenge excess O atoms [11], [12], therefore, some cases were run with $NO_2$ injected downstream of the discharge. The $NO_2$ injector ring was located 17.8 cm downstream from the exit of the longitudinal discharge. The $I_2$ injector ring was located 63.5 cm downstream from the exit of the longitudinal discharge. A tertiary $N_2$ diluent injector ring was located 78.7 cm downstream from the exit of the longitudinal discharge. Details of these experiments are provided in the following sections.

*1) $O_2$–He–NO Discharge Experiments With $NO_2$ Injected Downstream:* The initial lasing experiments were run with 3.0 mmol/s of $O_2$ mixed with 16.0 mmol/s of He and 0.15 mmol/s of NO flowing through the RF discharge. For these initial lasing tests, a flow rate of 0.23 mmol/s $NO_2$ was used to scavenge excess O atoms. The $NO_2$ flow was accompanied by 2.0 mmol/s of carrier He diluent. The secondary stream consisted of $\approx$0.008 mmol/s of $I_2$ with 2.0 mmol/s of secondary He diluent. The tertiary flow was 38 mmol/s of cold $N_2$ gas at a temperature of $\approx$ 135 K. The pressures in the subsonic diagnostic duct and in the supersonic diagnostic cavity were 10.4 and 1.35 torr, respectively.

Gain for the above flow conditions at 450-W RF discharge power is shown in Fig. 2 and peaks at 0.0067% cm$^{-1}$ at line center. The laser resonator was subsequently installed around the supersonic flow cavity and simultaneous measurements of $O_2(a)$

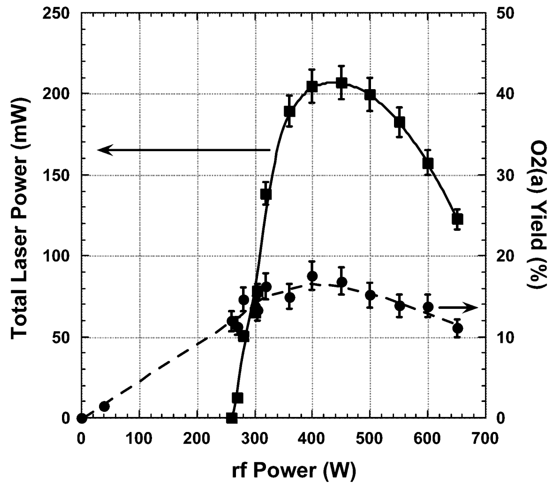


Fig. 3. $O_2(a)$ yield in the subsonic diagnostic section and total outcoupled laser power in the supersonic cavity as a function of RF discharge power. Subsonic flow tube pressure of 10 torr.

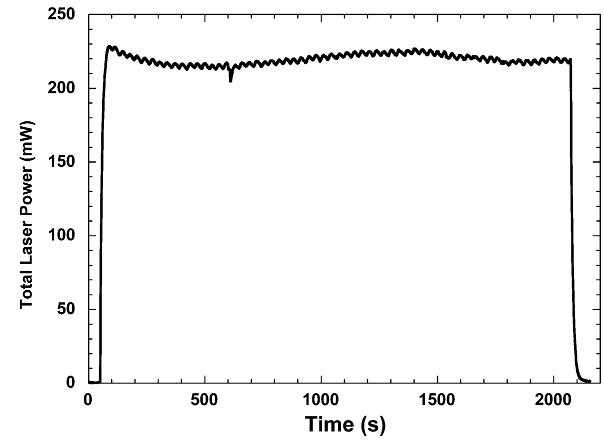


Fig. 4. Continuous wave (CW) outcoupled laser power as a function of time.

yield and laser power were made using two 1 m concave mirrors with a reflectivity of ≈ 0.99986, mirrors 1 and 2 from Table I. For the above flow conditions and 450-W RF power, a laser output power of 178 mW was obtained. The yield of $O_2(a)$ was ≈16% with a temperature of ≈410 K in the subsonic diagnostic duct (upstream of the $N_2$ diluent injection) and a temperature in the supersonic cavity of ≈ 180 K from the lineshape measurement. The beam shape was circular with a diameter of ≈1.9 cm, the same as the clear aperture of the mirror mounts. For reference, the first measurement of laser action using a classic liquid chemistry COIL system produced 4 mW [1].

*2) $O_2$-He–NO Discharge Experiments Without $NO_2$ Downstream:* Three sets of experiments were run with the longitudinal RF discharge with NO in the discharge and without $NO_2$ downstream of the discharge. The conditions used in the first set of these experiments were 3.0 mmol/s of $O_2$ mixed with 16.0 mmol/s of He and 0.15 mmol/s of NO flowing through the RF discharge. The secondary stream consisting of ≈ 0.008 mmol/s of $I_2$ with 2.0 mmol/s of He diluent was injected 63.5 cm downstream from the exit of the discharge. A tertiary flow of 55 mmol/s of cold $N_2$ gas (≈ 120 K) was injected further downstream to lower the temperature and to raise the pressure to improve the supersonic nozzle performance. The pressures in the subsonic diagnostic duct and in the supersonic diagnostic cavity were 12.6 and 1.55 torr, respectively. For these conditions, no additional $NO_2$ was employed to scavenge excess O atoms; in fact, at this slightly higher pressure, adding $NO_2$ was deleterious to laser performance. The reason for this effect is not fully understood at the moment, but may be in part due to a lower O atom production or higher O atom loss rate at these higher pressure conditions.

Gain for the above flow conditions at slightly higher pressure and 450 W of RF discharge power is approximately the same as that from Section IV-A.1, shown in Fig. 2, and also peaks at 0.0067% $cm^{-1}$ at line center. The lineshape also indicates a temperature of ≈ 180 K. The laser resonator was subsequently installed around the supersonic flow cavity and simultaneous measurements of $O_2(a)$ yield and laser power were made as a function of RF discharge power as shown in Fig. 3. For the above flow conditions and 450-W RF power, a laser output power of 207 mW was obtained. The yield of $O_2(a)$ was ≈ 17% with a temperature of ≈ 410 K in the subsonic diagnostic duct. (Note that the drop in $O_2(a)$ signal beyond 400 W is believed to be a consequence of discharge instabilities such as thermal constriction that are visible in our discharge under these flow conditions [12]). The beam shape was also circular with a diameter of ≈ 1.9 cm, the same as the clear aperture of the mirror mounts.

The threshold for laser oscillation lasing occurs at 260 W of RF discharge power and an estimated $O_2(a)$ yield of 12% in the subsonic flow tube, as shown in Fig. 3. Note that there is a roll off in laser power beyond 450 W that is greater than the drop in $O_2(a)$ yield which is in part attributed to discharge instabilities (there are also increasingly complex plasma-kinetic effects that occur at higher powers). Even in the absence of discharge instabilities, laser oscillation would likely decrease at higher powers for these conditions as a consequence of two factors: 1) higher powers result in higher gas temperatures and consequently lower gain and 2) progressively more O atoms are generated at higher powers while the NO flow rate was optimized for 450 W. (An excess of O atoms have been found to quench the excited $I^*$ atom [12]). A long duration run time test was performed and the laser power was relatively stable at 220 ± 10 mW for more than 33 min, as shown in Fig. 4. The cause of the small oscillations in Fig. 4 with a period of approximately 33 s corresponds to small fluctuations in the iodine source temperature (kept at 83 °C ± 2 °C) and therefore is likely a consequence of small fluctuations in the iodine flow rate. A second long duration test was performed in which the RF power, and consequently the laser power, was cycled on and off, Fig. 5; the power was found to be stable to within ±2% over the 32-min test.

A second series of experiments were run for three different mirror sets having different reflectivities. The same flow conditions discussed above were used for these experiments. Simultaneous measurements of laser power, $O_2(a)$ yield, $O_2(b)$ signal, and subsonic temperature were made as a function of RF discharge power as shown in Figs. 6 and 7. For the above flow conditions a peak laser output power of 184 mW was obtained with the mirror #1/#2 combination, 219 mW with the mirror #1/#3 combination, and 234 mW with the mirror #3/#4 combination. The yield of $O_2(a)$ was ≈ 17% with a temperature of ≈ 410 K in the subsonic diagnostic duct for the peak power points. For

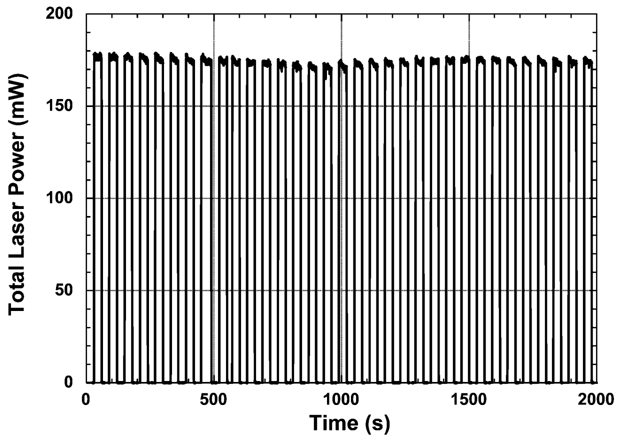

(a)

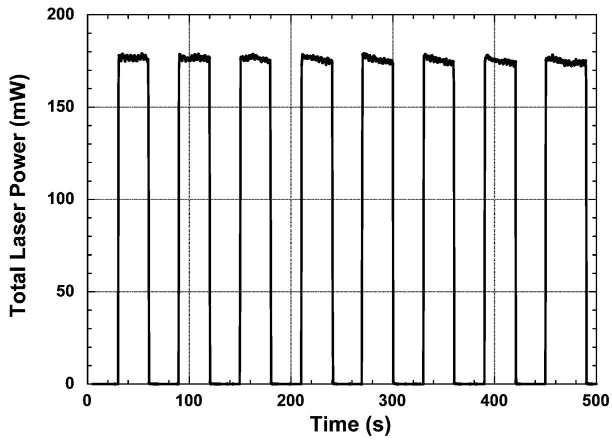

(b)

Fig. 5. CW cycled laser power as a function of time. (a) 32-min time scale. (b) Expanded 8-min time scale.

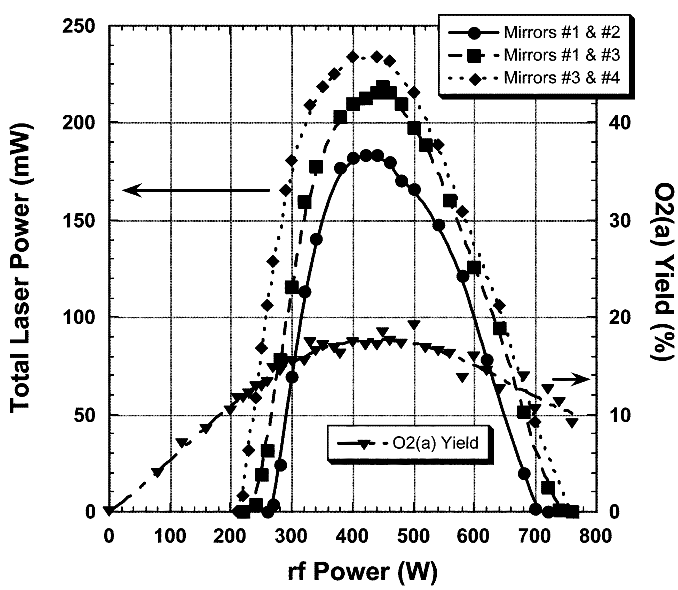


Fig. 6. $O_2(a)$ yield in the subsonic diagnostic section and total laser power in the supersonic cavity as a function of RF discharge power, for three different mirror sets. Subsonic flow tube pressure of 12.5 torr.

all but the low laser output power points, the beam shape was circular with a diameter of ≈ 1.9 cm, the same as the clear aperture of the mirror mounts. For the low laser output power data

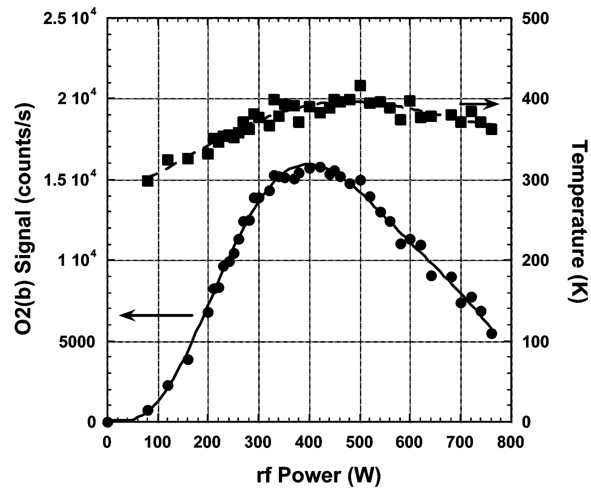


Fig. 7. $O_2(b)$ signal and flow temperature in the subsonic diagnostic section as a function of RF discharge power. Subsonic flow tube pressure of 12.5 torr.

the beam size was circular, but only a few millimters in diameter, which is probably a result of the highest gain region being in the core of the flow in the supersonic nozzle. The reasons for the drop in laser output power above 450 W of RF power are the same as discussed above for Fig. 3, i.e., discharge instabilities, higher temperature, and higher O atom production.

There are several interesting points to make from Fig. 6. First, the laser output power was always higher with the progressively higher reflectivity mirrors. Along similar lines, the laser threshold shifted to lower RF power as the reflectivity of the mirrors increased; this is consistent with the required threshold gain $\gamma_{\rm th}$ being smaller for higher reflectance mirrors (from Table I and (1), $\gamma_{\rm th} = 2.8 \times 10^{-5}$ cm$^{-1}$ for the #1/2 mirror set, $\gamma_{\rm th} = 2.1 \times 10^{-5}$ cm$^{-1}$ for the #1/3 mirror set, and $\gamma_{\rm th} = 1.4 \times 10^{-5}$ cm$^{-1}$ for the #3/4 mirror set) and that the $O_2(a)$ yield and gain decrease with lower RF power. In other words, the data support the expectation that higher reflective mirrors will lase at a lower value of gain. Note also that there is a variation in peak output power for the data presented in Figs. 3–6 all having approximately the same flow conditions and the same #1/#2 mirror set; we believe that the differences are primarily due to variations of a few degrees K in the day-to-day room temperature of the laboratory that consequently affected the vapor pressure of $I_2$ in the unheated $I_2$ sublimation cell.

Fig. 7 shows a drop in temperature above 500 W of RF power as measured by the $O_2(b)$ spectra; this was unexpected. It is believed that this may be a consequence of the flow volume viewed and the discharge instabilities (along with increasingly complex plasma-kinetic effects that occur at higher powers).

*3) $O_2$–He—NO Discharge Experiments Without $NO_2$ Injected Downstream and Varied $I_2$ Flow:* Post-discharge modeling of the experimental conditions discussed in Section IV-A.2 using the Blaze II kinetic/laser model [21] indicated that increasing the $I_2$ flow rate should improve gain and laser power (for brevity this modeling is not discussed in this paper). As such, experiments that varied the $I_2$ flow rate were performed. Other than the $I_2$ and the $I_2$ carrier gas (He) flow rates, all of the other flow conditions were the same as

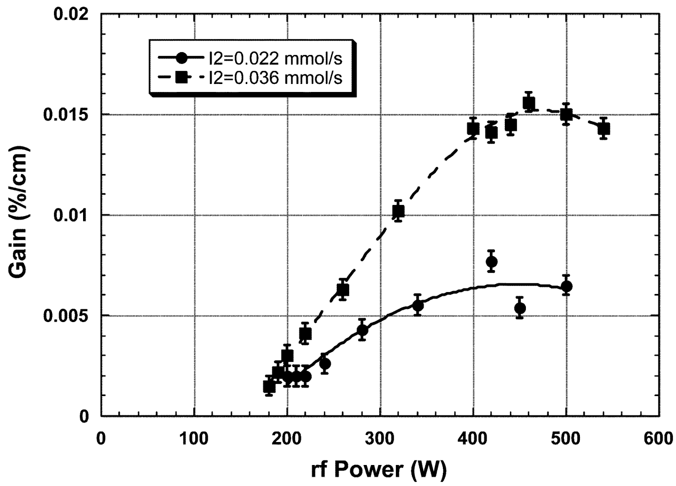


Fig. 8. Gain in the supersonic cavity as a function of RF discharge power, for two different iodine flow rates. Subsonic flow tube pressure of 12.5 torr.

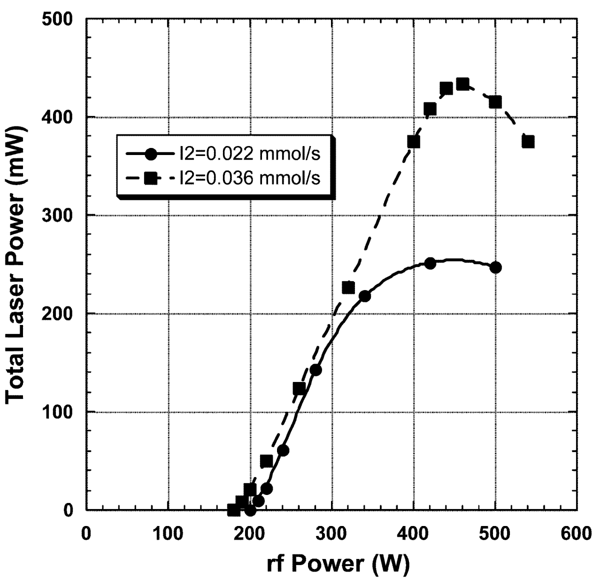


Fig. 9. Total outcoupled laser power in the supersonic cavity as a function of RF discharge power, for two different iodine flow rates. Subsonic flow tube pressure of 12.5 torr.

discussed in Section IV-A.2. First, the secondary flow rate of He was increased and was found to optimize laser power with a flow rate of 3.0 mmol/s of He rather than the 2.0 mmol/s used in Sections IV-A.1–2. The $I_2$ flow rate with a room temperature (25 °C) $I_2$ sublimation cell temperature and 3.0 mmol/s of secondary He was 0.014 mmol/s of $I_2$. The laser power with the #3 and #4 mirror set (relatively high reflectivity) increased to 260 mW.

To obtain further increases in the iodine flow rate the iodine sublimation cell was heated. With a 3.0 mmol/s secondary flow rate of He, the $I_2$ flow rate at $\approx$ 30 °C was approximately 0.022 mmol/s, at $\approx$ 40 °C the $I_2$ flow rate was approximately 0.036 mmol/s, and at $\approx$ 50 °C the $I_2$ flow rate was approximately 0.052 mmol/s. The power optimized around an $I_2$ flow rate of 0.040 mmol/s. Small signal gain and laser power measurements were made for the $I_2$ flow rates of 0.022 and 0.036 mmol/s cases as a function of RF power (Figs. 8 and 9). The laser measurements were made using the #3/#4 mirror set.

Fig. 8 shows that the gain increased substantially with the higher iodine flow rate, going from a peak of approximately 0.0077% $cm^{-1}$ to 0.0156% $cm^{-1}$, roughly a factor of two increase in gain. This result is consistent with the significantly higher laser power that was measured for the 0.036 mmol/s of $I_2$ case, Fig. 9. The total laser power that was measured for the 0.036 mmol/s of $I_2$ case was 440 mW. A few additional measurements produced as high a power as 510 mW for a slightly higher $I_2$ flow rate of 0.040 mmol/s. The lineshapes from the gain profiles (not illustrated for brevity) indicated laser cavity temperatures of $\approx$ 160 K for the 0.022 mmol/s $I_2$ case and $\approx$ 190 K for the 0.036 mmol/s $I_2$ case. Note that a higher $I_2$ flow rate should result in more heat release from chemical reactions, consistent with the lineshapes that indicated a higher temperature with more $I_2$ flow.

If we extrapolate the gain versus RF power curves back to optical transparency (zero gain) on Fig. 8, we find that both curves intersect zero gain at approximately 160 W of RF power. Knowing the temperature, we can make an estimate of the $O_2(a)$ yield in the supersonic cavity at this position using $Y_{\mathrm{OT}} = 1/[1 + 1.5\exp(403/T)]$ [20]. For temperatures of 160 and 190 K, the yields for optical transparency are 5.1% and 7.4% in the supersonic cavity, respectively. From Fig. 6, the yield in the subsonic region at 160 W is approximately 8.5%, so there is a drop in yield as the flow goes downstream from the subsonic diagnostic duct. Observe that the yield in the supersonic cavity at 160 W of RF power is approximately 5.1% with 0.022 mmol/s of $I_2$ and 7.4% with 0.036 mmol/s of $I_2$, i.e., a lower yield with lower $I_2$ flow. This observation seems counter-intuitive because one would *a priori* expect a lower yield with higher $I_2$ flow rate in a classic COIL device. A possible explanation for this phenomenon is that there may still be a significant excess of O atoms in the lower $I_2$ flow rate case, while the higher $I_2$ flow rate case more efficiently removes O atoms during the $I_2$ dissociation process

$$I_2 + O \rightarrow IO + I \tag{4}$$

$$IO + O \rightarrow O_2 + I \tag{5}$$

thereby leaving significantly fewer O atoms to quench the $I^*$ state via

$$I^* + O \rightarrow I + O. \tag{6}$$

Note that every $I_2$ molecule removes two O atoms through reactions (4) and (5). These reactions were found to play critical roles in the earlier gain demonstrations [11], [12].

*4) $O_2$–He Discharge Experiments Without NO and With $NO_2$ Injected Downstream:* Because NO was found to enhance the production of $O_2(a)$ by approximately 30%–50% when run through the discharge, [12] a very limited number of experiments were performed without NO in the discharge. Using the #3 and #4 mirror combination, a total of 132 mW of outcoupled laser power was measured with zero NO flow and an $NO_2$ flow rate of 0.35 mmol/s. The $I_2$ flow rate was approximately 0.027 mmol/s. Other than the NO, $NO_2$, and $I_2$ flow rates, all of the other flow conditions were the same as discussed in Section IV-A.2. Note that when zero NO and zero $NO_2$ were used that we were unable to obtain lasing. While lasing was demonstrated without NO in the discharge and with $NO_2$ added downstream to remove excess atomic oxygen, the performance was worse without NO in the discharge in all cases.

*5) $O_2$–He–$NO_2$ Discharge Experiments Without $NO_2$ Injected Downstream:* Because NO was found to enhance the production of $O_2(a)$ when run through the discharge, we decided to examine the substitution of $NO_2$ for NO in the discharge. The performance optimized with an $NO_2$ flow rate of 0.35 mmol/s flowing through the discharge with the $O_2$ and He (without any NO flow), but the peak $O_2(a)$ yield in the subsonic region was only approximately 11%, and the total outcoupled power was 132 mW using the #3 and #4 mirror combination. The $I_2$ flow rate was approximately 0.034 mmol/s. Other than the NO, $NO_2$, and $I_2$ flow rates, all of the other flow conditions were the same as discussed in Section IV-A.2. While moderate performance was demonstrated with $NO_2$ in the discharge, the performance was significantly worse than the results with NO in the discharge.

### *B. Laser Performance With an Inductive RF Discharge*

The second type of discharge tested was an inductively coupled RF discharge at 13.56 MHz in which the power was delivered to the discharge gas mixture through an inductive coil that surrounded the 4.9 cm inside diameter tube. This coil had five turns, was approximately 6.4 cm long in the flow direction, and had a resistive component of $\approx$ 0.46 $\Omega$. The inductive discharge had a plasma zone that was approximately 4.9 cm in diameter and 15–25 cm long (depending upon the amount of electric power deposited into the plasma, but always following the trend of a longer plasma zone with higher power); some details of the performance of this inductive discharge can be found in Verdeyen *et al.* [22].

*1) $O_2$–He–NO Discharge Experiments Without $NO_2$ Downstream:* Measurements of $O_2(a)$, $O_2(b)$, and laser power were made with the inductive discharge. The flow conditions were the same as those discussed in Section IV-A.3, with an $I_2$ flow rate of $\approx$ 0.035 mmol/s. It was found that the inductive discharge gave approximately the same $O_2(a)$ yield, Fig. 10, and $O_2(b)$ signal strengths as the longitudinal discharge [note that for brevity the $O_2(b)$ data is not illustrated]. At 400 W of RF power, the total laser power was approximately 524 mW using the #7/#8 mirrors. (Note that the #7/#8 mirror combination was our highest reflectivity pair of mirrors, Table I.)

*2) $O_2$–Ar–NO Discharge Experiments Without $NO_2$ Downstream:* In previous experiments with Ar diluent we have seen significantly worse $O_2(a)$ signals and yields with these types of discharges in our flow tube arrangement [5]. However, Ar is still an attractive diluent because it is less expensive than He and it is easier to pump than He. Therefore, some experiments were performed to establish the laser performance with Ar.

Fig. 11 shows the $O_2(a)$ yield in the subsonic diagnostic section as a function of RF power with the inductive discharge, for different discharge diluents and pressures. In all cases there was a flow of 3 mmol/s of $O_2$, 16 mmol/s of diluent (either He or Ar), and 0.15 mmol/s of NO through the discharge section. Two pressures were investigated, 12.5 and 20 torr. As in previous studies [5] we found that the He performance was significantly higher than that with Ar. But, interestingly, the yield for the two

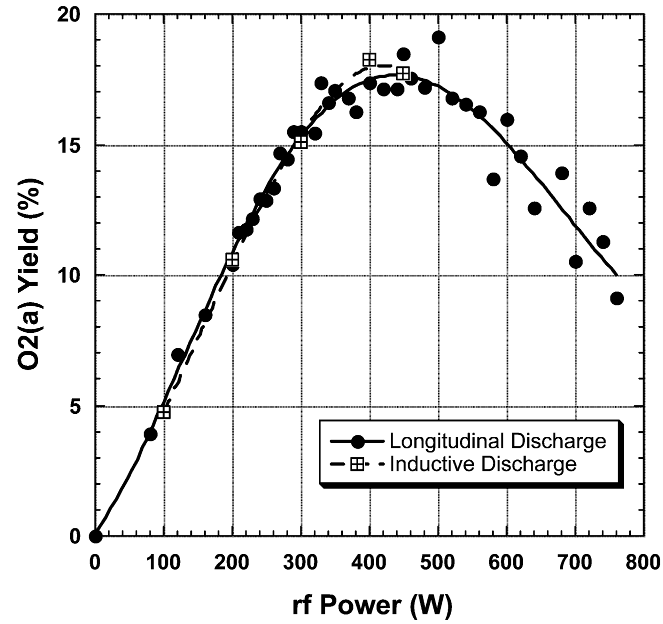


Fig. 10. $O_2(a)$ yield in the subsonic diagnostic section as a function of RF discharge power, for the longitudinal and the inductive discharges. Subsonic flow tube pressure of 12.5 torr.

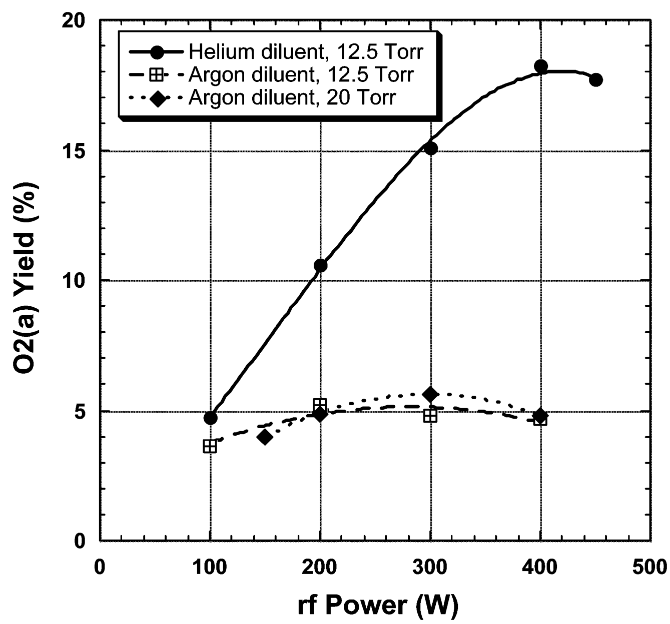


Fig. 11. $O_2(a)$ yield in the subsonic diagnostic section as a function of RF power with the inductive discharge, for different discharge diluents and pressures. In all cases there was a flow of 3 mmol/s of $O_2$, 16 mmol/s of diluent (either He or Ar), and 0.15 mmol/s of NO through the discharge section.

Ar pressure cases was approximately the same as the pressure increased, which is contrary to microwave excitation data reported by Rawlins *et al.* [23] that showed a decrease in yield as the partial pressure of $O_2$ increased (though it should be noted that Rawlins *et al.* worked in a pressure regime approximately an order of magnitude lower than our regime).

The total outcoupled laser power for the He diluted case peaked at 524 mW with the #7/#8 mirror combination and 400 W of RF power. With the same mirrors, zero laser power was observed with Ar diluent at 12.5 torr, however, 29 mW of

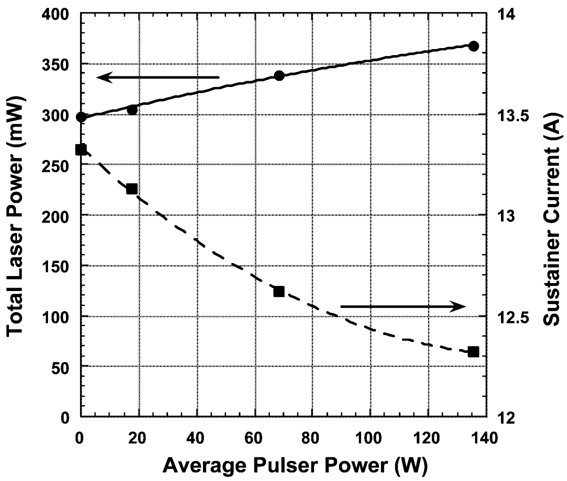


Fig. 12. Total laser power and current through the coil of the inductive sustainer as a function of the average pulser power.

laser power was observed with Ar diluent at 20 torr and 400 W of RF power. It is interesting that lasing was observed at 20 torr, but not 12.5 torr for the Ar diluted case when both have approximately the same yield of $O_2(a)$, Fig. 11. We believe that the explanation for this is simply that the higher pressure case has a significantly higher flow rate of cold tertiary $N_2$ ($\approx$ 35 mmol/s for the 12.5 torr case, and $\approx$ 93 mmol/s for the 20-torr case), thereby lowering the stagnation temperature of the flow and consequently the temperature in the supersonic cavity. With a lower temperature, the yield for optical transparency is lower and, hence, positive gain and lasing occurred for the higher pressure case, but not the lower pressure case.

Various mixes of 3 mmol/s of $O_2$ with a total of 16 mmol/s of He and Ar were also tested through the discharge. The results all at a pressure of 12.5 torr indicated a monotonic trend toward better $O_2(a)$ yield production with more He and less Ar in the discharge section.

### C. Experiments With Pulser-Sustainer Discharge

It has been has been suggested by Carroll *et al.* [24], Hill [7], [25], [26], King *et al.* [27], and Ionin [8] that a combination of a pulsed discharge to initiate high concentrations of electrons in conjunction with a sustained electric field to maintain the electron density between pulses may be a method of controlling the critical $E/N$ parameter, and thus enabling more of the electrical energy into the desired $O_2(a)$ state. As such, a third type of discharge tested was a combination of a high frequency, bipolar, high-voltage (HV) pulser combined with the RF inductive coil discharge as a "sustainer," to create a "pulser-sustainer" discharge. The pulse repetition rate of the bipolar pulser was 100 kHz, with a pulse length of 0.5 $\mu$s, and a variable peak power as discussed below. The pulsed discharge was conducted through the same longitudinal hollow cathodes discussed previously via a 5:1 transmission line transformer, and thus the plasma zone of this third type of discharge between the hollow cathodes was approximately 4.9 cm in diameter and 25 cm long.

Fig. 12 shows the total laser power and the current through the inductive coil sustainer as a function of the dc power supplied to drive the pulse. The flow conditions were similar to those discussed in Section IV-A.2, with an $I_2$ flow of approximately 0.025 mmol/s. As power is added to the pulser the laser power increases. Significantly, as power is added to the pulser the current through the sustainer coil decreases. Since the electric field $E_\phi$ from the inductive coil is proportional to the current I, as I decreases, then so must $E_\phi$ and consequently $E_\phi/N$. This is encouraging as it shows the desired trend, i.e., that of lowering $E_\phi/N$ with the addition of the pulser.

These are early results with the pulser-sustainer and are presented as proof of concept. To better understand the performance of this more complex discharge system a great deal more work needs to be done.

## V. Conclusion

In conclusion, CW laser action was measured on the $I^* \rightarrow I$ electronic transition of the iodine atom at 1315 nm pumped by a near resonant energy transfer from $O_2(a)$ produced in an electric discharge. A tertiary cold gas injection followed by expansion in a supersonic cavity was employed to lower the temperature of the flow and shift the equilibrium of atomic iodine in favor of the $I^*$ state. This produced sufficient population inversion to observe gains of as high as $\approx 0.015\%$ cm$^{-1}$. Laser oscillations were obtained for differing flow conditions and discharge arrangements when two high reflectivity mirrors were used to form an optical resonator surrounding the gain medium. Lasing was achieved under a variety of flow conditions.

1) An $O_2$–He–NO mixture running through the discharge and with $NO_2$ added downstream to remove excess atomic oxygen.
2) An $O_2$–He mixture running through the discharge with $NO_2$ added downstream to remove excess atomic oxygen.
3) An $O_2$–He–NO mixture running through the discharge in the absence of $NO_2$ added downstream.
4) An $O_2$–He–$NO_2$ mixture running through the discharge in the absence of $NO_2$ added downstream.
5) An $O_2$–Ar–NO mixture running through the discharge in the absence of $NO_2$ added downstream.

Laser oscillation was also achieved with three different discharge configurations: 1) a longitudinal RF discharge; 2) an inductive RF discharge; and 3) a pulser-sustainer configuration in which a bipolar HV pulser was combined with an inductive RF sustainer discharge. The highest laser output power obtained in these experiments was 520 mW in a stable cavity composed of two $\approx$ 99.995% reflective mirrors. One set of experiments demonstrated a laser output power of 220 mW that was stable for more than 30 min, and another set of experiments demonstrated the ability to cycle the electrical power on and off to produce repeatable laser power over a 30-min period.

## Acknowledgment

The authors would like to acknowledge the contributions of: T. Madden and G. Hager (Air Force Research Laboratory); M. Kushner and D. S. Stafford (University of Illinois at Urbana-Champaign); S. Davis, T. Rawlins and B. Kessler (Physical Sciences, Inc.); M. Heaven and K. Morokuma (Emory University); G. Perram (Air Force Institute of Technology); M. Berman (AFOSR); J. Mulroy (MDA); B. Otey (USA

SMDC); D. Baer (Los Gatos Research); A. Ionin (P.N. Lebedev Physics Institute); A. Napartovich (Troitsk Institute for Innovation and Fusion Research); and T. Rakhimova (Lomonosov Moscow State University). They would also like to thank T. Field for his technical assistance.

## REFERENCES

[1] W. McDermott, N. Pchelkin, D. Benard, and R. Bousek, "An electronic transition chemical laser," *Appl. Phys. Lett.*, vol. 32, no. 8, pp. 469–470, 1978.

[2] V. Zalesskii and Z. Yu, "A discharge laser operating on the iodine 1315-nm transition," *Eksp. Teor. Fiz.*, vol. 67, pp. 30–37, 1974.

[3] G. Fournier, J. Bonnet, and D. Pigache, "A potential atomic iodine laser pumped by electrically generated $^1\Delta$ oxygen," *J. Physique*, vol. 41, p. 449, 1980.

[4] D. L. Carroll, J. T. Verdeyen, D. M. King, B. S. Woodard, L. W. Skorski, J. W. Zimmerman, and W. C. Solomon, "Modeling of the ElectriCOIL System," *IEEE J. Quantum Electron.*, vol. 39, no. 9, pp. 1150–1159, 2003.

[5] D. L. Carroll, J. T. Verdeyen, D. M. King, B. S. Woodard, J. W. Zimmerman, L. W. Skorski, and W. C. Solomon, "Recent experimental measurements of the ElectriCOIL system," presented at the AIAA 34th Plasmadynamics and Lasers Conf., Orlando, FL, Jun. 2005, Paper no. 2003–4029.

[6] J. Schmiedberger, S. Hirahara, Y. Ichinoche, M. Suzuki, W. Masuda, Y. Kihara, E. Yoshitani, and H. Fujii, "RF plasma jet generator of singlet delta oxygen for oxygen–iodine laser," *Proc. SPIE*, vol. 4184, pp. 32–35, 2001.

[7] A. E. Hill, "The next generation of controlled avalanche discharge lasers—including an extension to the electric oxygen iodine laser," in *Proc. Int. Conf. Lasers 2000*, V. Corcoran and T. Corcoran, Eds., McClean, VA, 2001, pp. 249–258.

[8] A. A. Ionin, Y. M. Klimachev, A. A. Kotkov, I. V. Kochetov, A. P. Napartovich, L. V. Seleznev, D. V. Sinitsyn, and G. D. Hager, "Non-self-sustained electric discharge in oxygen gas mixtures: Singlet delta oxygen production," *J. Phys. D: Appl. Phys.*, vol. 36, pp. 982–989, 2003.

[9] T. V. Rakhimova, A. S. Kovalev, A. T. Rakhimov, K. S. Klopovsky, D. V. Lopaev, Y. A. Mankelevich, O. V. Proshina, O. V. Braginsky, and A. N. Vasilieva, "Radio-Frequency plasma generation of singlet $(a^1\Delta_g)$ oxygen in $O_2$ and $O_2$:Ar (He) mixtures," presented at the AIAA 34th Plasmadynamics and Lasers Conf., Orlando, FL, Jun. 2005, Paper no. 2003–4306.

[10] D. S. Stafford and M. J. Kushner, "$O_2(^1\Delta)$ production in He/$O_2$ mixtures in flowing low pressure plasmas," *J. Appl. Phys.*, vol. 96, no. 5, pp. 2451–2465, 2004.

[11] D. L. Carroll, J. T. Verdeyen, D. M. King, J. W. Zimmerman, J. K. Laystrom, B. S. Woodard, N. Richardson, K. Kittell, M. J. Kushner, and W. C. Solomon, "Measurement of positive gain on the 1315 nm transition of atomic iodine pumped by $O_2(a^1\Delta)$ produced in an electric discharge," *Appl. Phys. Lett.*, vol. 85, no. 8, pp. 1320–1322, 2004.

[12] D. L. Carroll, J. T. Verdeyen, D. M. King, J. W. Zimmerman, J. K. Laystrom, B. S. Woodard, G. F. Benavides, K. Kittell, and W. C. Solomon, "Path to the measurement of positive gain on the 1315 nm transition of atomic iodine pumped by $O_2(a^1\Delta)$ produced in an electric discharge," *IEEE J. Quantum Electron.*, vol. 41, no. 2, pp. 213–223, Feb. 2005.

[13] D. L. Carroll, J. T. Verdeyen, D. M. King, J. W. Zimmerman, J. K. Laystrom, B. S. Woodard, G. F. Benavides, K. Kittell, D. S. Stafford, M. J. Kushner, and W. C. Solomon, "Continuous-wave laser oscillation on the 1315 nm transition of atomic iodine pumped by $O_2(a^1\Delta)$ produced in an electric discharge," *Appl. Phys. Lett.*, vol. 86, pp. 111 104–1–3, 2005.

[14] W. T. Rawlins, S. Lee, W. J. Kessler, and S. J. Davis, "Observations of gain on the $I(^2P_{1/2} \rightarrow {}^2P_{3/2})$ transition by energy transfer from $O_2(a^1\Delta_g)$ generated by a microwave discharge in a subsonic-flow reactor," *Appl. Phys. Lett.*, vol. 86, pp. 051 105–1–3, 2005.

[15] W. T. Rawlins, S. J. Davis, S. Lee, M. L. Silva, W. J. Kessler, and L. G. Piper, "Optical diagnostics and kinetics of discharge-initiated oxygen–iodine energy transfer," presented at the AIAA 34th Plasmadynamics and Lasers Conf., Orlando, FL, Jun. 2005, Paper no. 2003–4032.

[16] S. J. Davis, M. G. Allen, W. J. Kessler, K. R. McManus, M. F. Miller, and P. A. Mulhall, "Diode laser-based sensors for chemical oxygen iodine lasers," *Proc. SPIE*, vol. 2702, pp. 195–201, 1996.

[17] G. D. Hager, private communication, Oct. 25, 2002.

[18] R. G. Derwent and B. A. Thrush, "Excitation of iodine by singlet molecular oxygen," *Discuss. Faraday Soc.*, vol. 53, pp. 162–167, 1972.

[19] G. P. Perram and G. D. Hager, "The standard COIL kinetics package," Air Force Weapons Lab., Kirtland Air Force Base, Final Rep. AFWL-TR-88-50, 1988.

[20] J. Hon, G. Hager, C. Helms, and K. Truesdell, "Heuristic method for evaluating coil performance," *AIAA J.*, vol. 34, no. 8, pp. 1595–1603, 1996.

[21] L. Sentman, M. Subbiah, and S. Zelazny, "Blaze II: A chemical laser simulation computer program," Bell Aerospace Textron, Buffalo, NY, Tech. Rep. H-CR-77-8, 1977.

[22] J. T. Verdeyen, D. M. King, D. L. Carroll, and W. C. Solomon, "Diagnostic development for the ElectriCOIL flow system," *Proc. SPIE*, vol. 4631, pp. 154–160, 2002.

[23] W. T. Rawlins, S. Lee, W. J. Kessler, D. B. Oakes, L. G. Piper, and S. J. Davis, "Spectroscopic studies of a prototype electrically pumped COIL system," *Proc. SPIE*, vol. 5334, pp. 88–99, 2004.

[24] D. L. Carroll, J. T. Verdeyen, and W. C. Solomon, "Method, system and apparatus for an electrically assisted chemical oxygen iodine laser," U.S. Patent 6 501 780, Dec. 31, 2002.

[25] A. E. Hill, "Electric oxygen iodine laser," U.S. Patent 6 826 222, Nov. 30, 2004.

[26] ——, "Laser plasma electrical excitation methods: Their properties, techniques, and specific applications," *Proc. SPIE*, vol. 4747, pp. 23–30, 2002.

[27] D. M. King, D. L. Carroll, J. K. Laystrom, J. T. Verdeyen, M. S. Sexauer, and W. C. Solomon, "ElectriCOIL: Preliminary experiments of excited oxygen generation by RF discharge," in *Proc. Int. Conf. Lasers 2000*, V. Corcoran and T. Corcoran, Eds., McClean, VA, 2001, pp. 265–272.

[28] D. L. Carroll, "Modeling high-pressure chemical oxygen–iodine lasers," *AIAA J.*, vol. 33, no. 8, pp. 1454–1462, 1995.

[29] H. Schlichting, *Boundary Layer Theory*, 7th ed. New York: McGraw-Hill, 1979, p. 141.

[30] ——, *Boundary Layer Theory*, 7th ed. New York: McGraw-Hill, 1979, p. 186.

**David L. Carroll** (M'97) was born in Princeton, NJ. He received the B.S., M.S., and Ph.D. degrees in aeronautical and astronautical engineering from the University of Illinois at Urbana-Champaign (UIUC) in 1985, 1986, and 1992, respectively.

He is the founder and Engineering Director of CU Aerospace, Champaign, IL. Other positions he has held through the years include: Member of Technical Staff with TRW, Redondo Beach, CA, from 1987 to 1988; Postdoctoral Research Associate with UIUC from 1992 to 1995; Research Scientist with UIUC from 1995 to 2000; and Adjunct Lecturer with UIUC in 2001. He has performed in-depth chemical laser system research for 20 years including HF and COIL performance and modeling, materials processing experiments with COIL, and issues related to the commercialization of these devices. He has also performed research on stimulated Brillouin scattering beam combination and genetic algrithms. His current research is focused on the development of the electrically assisted oxygen–iodine laser.

**Joseph T. Verdeyen** (M'63–SM'74–LS'96) was born in Terra Haute, IN. He received the B.S.E.E. degree from Rose-Hulman Institute of Technology, Terra Haute, IN, in 1954, the M.S. degree from Rutgers University, New Brunswick, NJ, in 1958, and the Ph.D. degree in electrical engineering from the University of Illinois at Urbana-Champaign (UIUC) in 1962.

He served with the U.S. Army from 1955 to 1957, was Director of the UIUC Gaseous Electronics Laboratory from 1972 to 1974, was Director of the Compound Semiconductor Microelectronics Laboratory and the National Science Foundation Center for Compound Semiconductor Microelectronics from 1988 to 1989, has been a Professor Emeritus with the University of Illinois since 1994, and consults as a Senior Scientist to CU Aerospace, Champaign, IL. After undergraduate studies, he worked for Bell Telephone Laboratories, Murray Hill, NJ. After completing his graduate studies, he remained at the University of Illinois as a Faculty Member in Electrical and Computer Engineering. He has been a consultant to Zenith and Lucitron on plasma display technology, General Electric at Nela Park and Applied Physical Laboratories on Lighting, Protech and TEL on RF discharges and plasma processing, and Sandia and Livermore National Laboratories on microwave and RF discharges. His current research interests are lasers (gas, solid-state, and semiconductor), optical communications and control, plasma display technology, and gas-phase processing of materials.

**Darren M. King** was born in Belleville, IL. He received the B.S. and M.S. degrees from the University of Illinois at Urbana-Champaign (UIUC) in 1996 and 1999, respectively. His M.S. thesis was on extensive experimental research with the VertiCOIL device.

He is currently a Staff Engineer with CU Aerospace, Champaign, IL, and works with chemical lasers, electronics, power systems, controls, and data acquisition. He has a diverse experimental background and has participated in systems-level as well as component-level design work and testing on chemical lasers, electric propulsion systems, and chemical rockets.

**Joseph W. Zimmerman** was born in Elmhurst, IL, in 1979. He received the B.S. and M.S. degrees in aeronautical and astronautical engineering from the University of Illinois at Urbana-Champaign (UIUC) in 2001 and 2003, respectively.

His graduate research involved the modeling of gas discharges for use in oxygen–iodine lasers. Currently, he is a Staff Engineer with CU Aerospace, Champaign, IL, performing experimental investigations on the electrically assisted oxygen–iodine laser.

**Julia K. Laystrom** was born in Elgin, IL, in 1977. She received the B.S. degree in aeronautical and astronautical engineering and the M.S. degree in aerospace engineering from the University of Illinois at Urbana-Champaign (UIUC) in 1999 and 2004, respectively. Her M.S. thesis and graduate research focused on studying, designing, and testing pulsed plasma thrusters for electric satellite propulsion.

Following the B.S. degree, she worked for CU Aerospace, Champaign, IL, as a Staff Engineer in the electric propulsion and chemical laser laboratories. She then returned to UIUC for her master's work. She has returned to CU Aerospace as a Staff Engineer and is currently contributing to the electrically assisted oxygen–iodine laser project.

**Brian S. Woodard** was born in Harristown, Illinois. He received his B.S. in Aerospace Engineering in 2001 from the University of Illinois at Urbana-Champaign (UIUC). He then worked for the Department of Aerospace Engineering as a Visiting Academic Professional until the fall of 2002. He then began pursuing the M.S. degree in Aerospace Engineering at UIUC which he completed in 2004. During his academic and professional careers he has developed and conducted laboratory experiments with the goal of creating an electrically assisted oxygen–iodine laser.

**Gabriel F. Benavides** was born in St. Louis, MO. He received the B.S. degree in aeronautical and astronautical engineering from the University of Illinois at Urbana-Champaign (UIUC) in 2001, where he is currently working toward the M.S. degree in aerospace engineering.

After receiving his undergraduate degree, he joined CU Aerospace, Champaign, IL, as a Staff Engineer. He currently conducts experimental research, component-level design, and system-level design in the areas of chemical lasers and electric propulsion.

**Nathan R. Richardson** was born in Ft. Madison, Iowa. He received the B.S. and M.S. degrees in aerospace engineering from the University of Illinois in Champaign Urbana, in 2003 and 2005, respectively.

**Kirk W. Kittell** was born in Illinois. He received the B.S. degree in aerospace engineering from the University of Illinois at Urbana-Champaign in 2003, where he is currently working toward the M.S. degree in aerospace engineering.

His topic of research is the electrically assisted oxygen–iodine laser.

**Wayne C. Solomon** was born in Boise, ID. He received the B.S. degree from the University of Idaho, Pocatello, in 1956 and the Ph.D. degree from the University of Oregon, Portland, in 1963, both in chemistry.

He is currently a Professor Emeritus with the University of Illinois at Urbana-Champaign (UIUC). He was a Professor and former Head of the Department of Aeronautical and Astronautical Engineering at UIUC from 1988 to 2001. He is a founder and President of CU Aerospace, Champaign, IL, in 1998, was Director of Engineering at Bell Aerospace Textron from 1973 to 1988, a Staff Scientist with the Air Force at Edwards AFB from 1963 to 1967 and 1969 to 1973, and a Visiting Professor with the Institute fur Physikalische Chemie, Goettingen, from 1967 to 1969. He joined the faculty at the University of Illinois, Urbana, after directing all of the high-energy laser activities at Bell Aerospace Textron. His activities include research for several families of high-energy chemical lasers. Several laser systems which were significantly advanced under his leadership included DF-$CO_2$, HF space laser devices, DF lasers, and COIL devices. His current research includes ElectriCOIL and COIL laser technology with nitrogen diluent and large-scale CFD modeling of COIL devices.